International Journal of Research in Engineering, Science and Management
Volume-1, Issue-6, June 2018
www.ijresm.com

Jet Impingement on a Flat Plate with Different Plate Parameters

P. R. Sanjai

Student, Department of Mechanical Engineering, Universal Engineering College, Trissur, India

***Abstract*—The impingement of supersonic jets on solid objects create lot of problems arise in a wide variety of situations like gas-turbine blade failure, multistage rocket separation, lunar and planetary landing, deep-space docking, space-module attitude-control thrusters operation and take-off, jet-engine exhaust impingement, shock-impingement heating, gun-muzzle blast impingement and terrestrial rocket launch. The impingement flows are generally found to be extremely more complex. They contain mixed subsonic and supersonic regions, and expansion systems, highly non-uniform upstream flows, regions of turbulent shear and instances of major flow instabilities. This paper reports an investigation in which the impingement on a flat plate with different plate parameters by using CFD software. Plate inclinations at 80°, 70°, 60° were investigated with h/d (plates spacing to jet diameter ratio) =1, 2. The flows are shown to be extremely complex due to the local structure of the free jet and particularly, due to interactions between shock waves in the free jet and those created by the plate. These interactions tend to be the controlling factors but at larger distances from the nozzle, mixing effects become increasingly important. Here we discuss the static pressure distribution with different plate parameters.**

Index Terms— Jet impingement, flow visualization, CFD modelling

I. Introduction

The impinging jet can be defined as a high velocity coolant mass ejected from a hole impinges on a heat transfer surface. A characteristic feature of this flow arrangement is an intensive heat transfer rate between the fluid and the wall. It predetermined the fluid jets widely used in industrial applications where efficient heat transfer rate are needed. For example for cooling of turbine blades, laser mirrors and electronic components for paper drying, multistage rocket separation etc. The jet zone is situated directly beneath of the nozzle. The fluid issuing from the nozzle mixes with the quiescent surrounding fluid which creates a flow field. This flow field is up to a certain distance from the wall identical with the flow field of submerged non impinging jet. The jet flow is undeveloped up to six or seven nozzle diameters from the nozzle lip. Consequently, in most applications, the nozzle-to-plate distance is too small to enable the developed jet flow conduction. Then a shear layer forms around the jet. Its properties are depends strongly on the nozzle type. In most situations, except a laminar flow from a tube nozzle, the shear layer is initially relatively thin compared to the nozzle diameter. Therefore its dynamical behaviours are similar to that of a plane shear layer. The shear layer thickness becomes comparable with the jet diameter downstream, and the behaviour of the layer changes considerably [3].

Most rocket nozzles are of converging-diverging De Laval type. Since the flow velocity of the gases in the converging section of the rocket nozzle is relatively low, any smooth and well-rounded convergent nozzle section will have very low energy losses. The contour of the diverging nozzle section is very important to performance, because of very high flow velocities involved. To gain higher performance and shorter length the nozzle divergent has to be bell shaped [4].

II. Test Facility

Compressed air for the jets was supplied to the nozzles by Carling & Hunt's (1974) work. This is connected to a 30 bar main and incorporates a control valve and a settling chamber. The pressure in the chamber is displayed on a Budenberg test gauge. Early on in the work, it was found that acoustic reflexion from the base of the settling chamber produced unsteadiness in the impingement flows under some conditions .The base of the chamber was then covered with a thick layer of cotton padding, which acted as a sound absorber [1].

The convergent-divergent type nozzle is used with identical design downstream of the throat. This consists of an initial expansion in the form of a circular arc with radius equal to the throat diameter, which is 21.4 mm, and a conical exit section of 15° semi-angle. The exit diameter, Do is 30 mm, giving a design lip Mach number of 2.2. One of the nozzles, referred to here as the short nozzle is that used. It has an entry contraction whose final section is a circular arc of radius equal to 2.56 times the throat diameter. The other nozzle, referred to as the long nozzle, has an elliptical entry contour whose radius of curvature at the throat is 5.2 times the throat diameter [6].

III. Nozzle Design

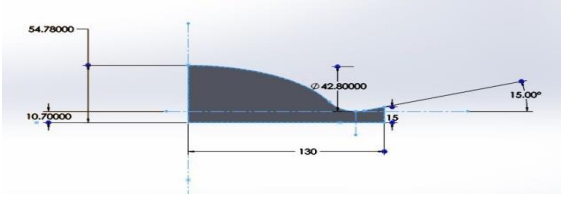

Fig. 1. Nozzle design

The convergent divergent nozzle with throat diameter of 21.4 mm and a conical exit section of ⟦15⟧^°semi-angle. Inlet diameter of the nozzle is 109.56mm, exit diameter of 30 mm and the length of the nozzle is 130 mm. The nozzle design shown as in the Fig. 1.

IV. Experimental Condition

The experimental conditions for the experiment are tabulated in the Table 1.

TABLE I
EXPERIMENTAL CONDITIONS

	Main Flow
Fluid	air
Mach number at exit of nozzle	2.2
Stagnation pressure (bar)	30
Stagnation temperature (k)	300
Mass flow rate (kg/s)	31.2

V. Computational Analysis

The numerical simulation is done in the commercial CFD software FLUENT. The validation has done for SST k-ω.

VI. Mesh Sensitivity

Mesh sensitivity study is carried out to ascertain the accuracy of the numerical results. The mesh sensitivity study is carried out by analyzing the mach number variation at the exit of the nozzle.

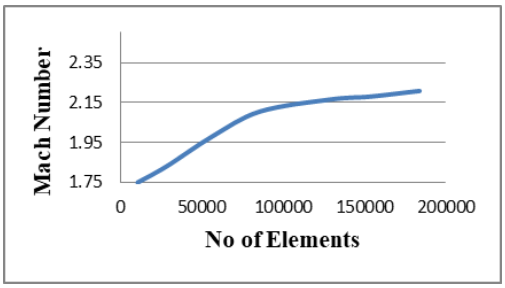

Fig.2. Variation of Mach number with number of elements

TABLE II
NUMERICAL RESULTS OF MACH NUMBER WITH CORRESPONDING MESH SIZE

Mesh size	Mach number
183827	2.221
153867	2.212
128678	2.165
85699	2.105
56387	1.98
28224	1.83
10574	1.75

It is clear from the Table 2, the difference in the value of mach number with mesh size. The results showed that the increase of grid size of183827does not yield any significant variation in the results. The study also showed that 80000 grids were quite insufficient to capture the flow in a refined manner and 153867 mesh was having slight deviations from the required mach number. Hence the grid size was finalized as 150000. Both structured and unstructured grids were used (120278 hexahedral grids). Similar mesh sensitivity study is done for all other cases. The Fig. 2. Show the graphical representation of mach number and number of elements. Meshing of size with 150000 is shown in Fig. 3.

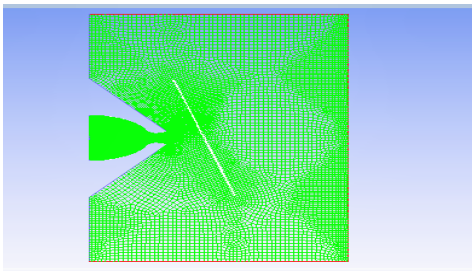

Fig. 3. Mesh

VII. Results and Discussion

The variations of static pressure distribution on different plate spacing to jet diameter ratio (h/d) with different plate angles are discussed here. The peak pressure is observed at the point of stagnation region of jet.

Pressure Contours at h/d=1 with 60°, 70°, 80°, 90°:

The pressure contour of plate spacing to jet diameter ratio (h/d) =1 at 60° plate angle is shown in Fig. 4.

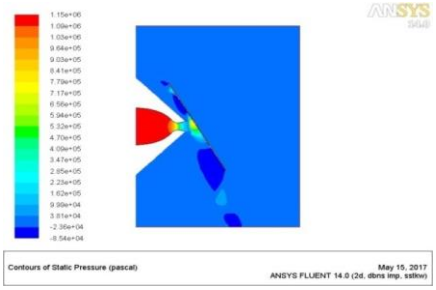

Fig. 4. Pressure contour of h/d =1 at 60°

The pressure at the middle of the plate is 5.92 bar. Two peak pressures are formed in the upstream side of the plate. The first peak has a pressure of 8.2 bar at a distance 10 mm in the upstream region and the second peak have a pressure of 3.2 bar at a distance 120 mm in the upstream region. But the pressure is reduced in the downstream region.

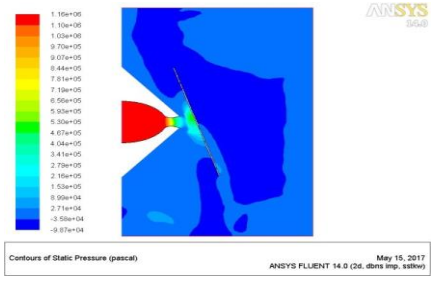

Fig. 5. Pressure contour of h/d =1 at 70°

The pressure contour of plate spacing to jet diameter ratio (h/d) =1 at 70° plate angle is shown in Fig. 5.

The maximum pressure obtained on the surface of the plate is 5.4 bar and there is no secondary peak is obtained here. The pressure contour of plate spacing to jet diameter ratio (h/d) =1 at 80° plate angle is shown in Fig. 6. The maximum pressure on the surface of the plate is 8 bar.

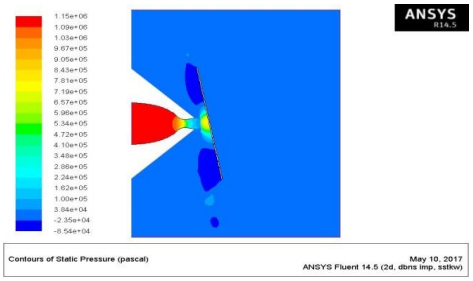

Fig. 6. Pressure contour of h/d =1 at 80°

Pressure Contours at h/d=2 at60°, 70°, 80°, 90°:

The pressure contour of plate spacing to jet diameter ratio (h/d) =2 at 60° plate angle is shown in Fig. 7. Here the two pressure peaks are obtained. The first peak has a pressure of 4 bar and the secondary peak has a value of 1 bar.

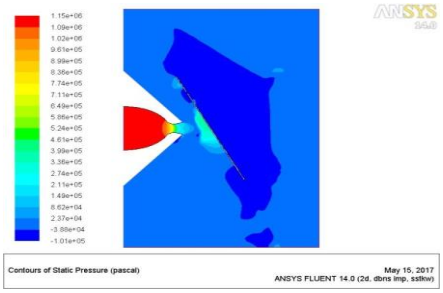

Fig. 7. Pressure contour of h/d =2 at 60°

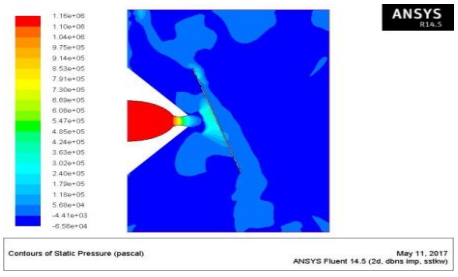

Fig. 8. Pressure contour of h/d =2 at 70°

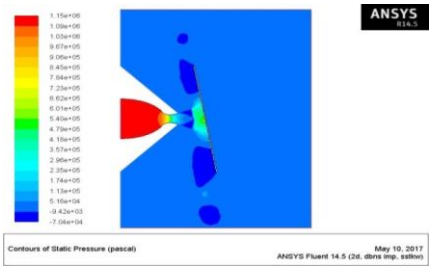

Fig. 9. Pressure contour of h/d =2 at 80°

The pressure contour of plate spacing to jet diameter ratio (h/d) =2 at 70° plate angle is shown in fig 8. The maximum pressure obtained on the surface of the plate is 3.6 bar.

The Fig. 9. Shows the pressure contour of h/d =2 at 80°. The maximum pressure obtained on the test plate is 5.8 bar.

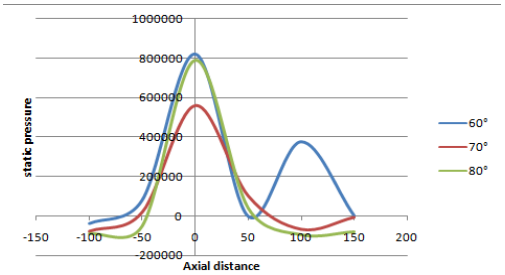

Fig. 10. Comparison of pressure at h/d=1 with 60°, 70°, 80°

The Fig. 10. Shows the pressure on a test plate obtained by the jet impingement at h/d=1 with 60°, 70°, 80°. It is clear that the secondary peak move towards the first peak by increasing the plate angle. The maximum pressure obtained at an angle of 60°.

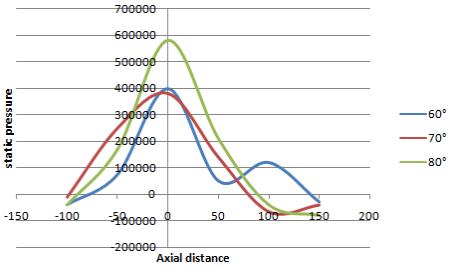

Fig. 11. Comparison of pressure at h/d=2 with 60°, 70°, 80°

The maximum pressure on the test plate obtained at h/d=2 is less than the pressure at h/d=1.The maximum pressure obtained is 5.8 bar at 80° plate angle. 40% of pressure is reduced by increasing the plate spacing to jet diameter ratio (h/d). The secondary peak is obtained at an angle 60°. But the secondary peak move towards the first peak by increasing the plate angle.

VIII. Conclusion

The flow structure is visualised using CDF software. Computationally obtained topology of flow pattern on the impingement surface is agree with the experiment. It is observed that the flow topology is altered with variation of h/d. The pressure distribution obtained from experiment is similar to computation. This validates the usage of shear stress transport (SST) (K-ω) turbulence model for the chosen problem. Peaks are noticed in primary and secondary stagnation region. Larger peaks are observed for lower h/d value of unity. The peaks are reduced by decreasing the plate angle and increasing plate spacing to jet diameter ratio h/d. The secondary peaks are move towards the centre jet by increasing the plate angle and plate spacing to jet diameter ratio h/d.

REFERENCES

[1] P. J. Lamont and B. L. Hunts, The impingement of under expanded, axisymmetric jets on perpendicular and inclined flat plates Department of Aeronautical Engineering, University of Bristol, England, J. Fluid Mech. (1980), vol100, part 3, pp. 471-611.

[2] K. Ravi Kumar, M.R.Ch. Sastry, K. Durga Prasad, International Journal of Engineering Research and Applications (IJERA), Vol. 2, Issue5, September- October 2012, pp.1976-1985.

[3] Makatar Wae-hayee, Perapong Tekasakul and Chayut Nuntadusit, Cross-flow Effect on Flow and Heat Transfer Characteristics of Impinging Jets in a Confined Channel, Engineering transactions, vol. 17, no.1 (36) Jan-June 2014.

[4] Neil Zuckerman and Noam Lior, Radial Slot Jet Impingement Flow and Heat Transfer on a Cylindrical Target, Journal of Thermophysics and Heat Transfer Vol. 21, No. 3, July-September 2007.

[5] Wael M. El Maghlany, Ahmed A. Hanafy, Khaled M. Abdou, Mohamed A. Teamah, Numerical Simulation for Confined Rectangular Slot Jets Impingement on Isothermal Horizontal Plate, European Journal of Scientific Research, Vol.76 No.4 (2012), pp.553-566, EuroJournals Publishing, Inc. 2012.

[6] Mehmet Baris Dogruoz, Experimental and Numerical Investigation of Turbulent Heat Transfer Due to Rectangular Impinging Jets, The University of Arizona (2005).

[7] Tadhg S. O Donovan , Darina B. Murray, Jet impingement heat transfer-Part I: Mean and root-mean-square heat transfer and velocity distributions, International Journal of Heat and Mass Transfer 50 (2007) 3291–3301.

[8] Nawaf H. Saeid, Effect of Oscillating Jet Velocity on the Jet Impingement Cooling of an Isothermal Surface, Engineering,2009.

[9] M.J. Remie, M.F.G. Cremers, K.R.A.M. Schreel, L.P.H. de Goey, Analysis of the heat transfer of an impinging laminar flame jet, International Journal of Heat and Mass Transfer 50 (2007) 2816–2827.

[10] N. Zuckerman and N. Lior, Jet Impingement Heat Transfer: Physics, Correlations, and Numerical Modelling, Advances in Heat Transfer Volume 39 (2006).

[11] Akshay R. Nangare and Dr. Uday S. Wankhede, Multiple Jet Impingement: A Promising Method of Cooling, IJLTET, Vol.6 Issue 4 March 2016.

[12] K Marzec and A Kucaba-Pietal, Heat transfer characteristic of an impingement cooling system with different nozzle geometry, Journal of Physics: Conference Series 530 (2014) 012038.